Femtosecond Laser Ionization of Organic Amines with Very Low Ionization Potentials: Relatively Small Suppressed Ionization Features

Tomoyuki Yatsuhashi,* Takashi Obayashi, Michinori Tanaka, Masanao Murakami, and Nobuaki Nakashima

Department of Chemistry, Graduate School of Science, Osaka City University, 3-3-138 Sugimoto, Sumiyoshi, Osaka 558-8585, Japan

Received: March 31, 2006; In Final Form: May 3, 2006

We examined the femtosecond nonresonant ionization of organic amines with vertical ionization potentials as low as 5.95 eV. The quantitative evaluation of suppressed ionization relative to the single active electron approximation model was done by comparing the saturation intensity, I_{sat}, in experiments and theory. ADK theory was found to be useful in predicting the ionization yield in the I_{sat} scale within a factor of 2, even for molecules with very low ionization potentials. The degree of suppression was, however, smaller than that of benzene. The localization of electrons on the nitrogen atom was found to affect the ionization behavior under the strong laser field. The delocalized π electrons in benzene could not follow the laser field adiabatically, while those in localized molecular orbitals could. In addition, the growth of a tunneling barrier due to the screening effect in amines may be relatively smaller than that in benzene.

Introduction

The interaction between a high intense femtosecond laser field and matter is one of the most attractive research subjects in laser chemistry.[1] The most fundamental process under a strong laser light field is ionization, and many interesting features have been found; however, the ionization of atoms (rare gases) and simple (diatomic) molecules have been the main focus of these studies. For instance, the exact time evolution of the electron wave packet dynamics of H_2 under an intense laser field was solved successfully.[2] On the other hand, understanding the ionization behavior of large molecules is more difficult due to their complexity. In many cases, the molecular ion does not survive; fragmentation of a molecular ion prevents us from comparing results with theoretical predictions. The importance of radical cations in the postionization fragmentation process has been increasingly recognized,[3] and controversy as to the fragmentation mechanism including nonadiabatic excitation is ongoing.[4,5] Evidently, we can use shorter duration pulse[6] and/or pulses at a suitable wavelength that is off-resonant with the molecular cation radicals to avoid fragmentation.[7,8] Besides fragmentation, the suppression of ionization is one of the recent important topics in molecular ionization studies and has attracted the attentions of both experimentalists and theorists. Generally speaking, molecules are hard to ionize (the ionization rate is smaller than that of rare gases with the same ionization potential) although the difference in ionization rate has remained unexplained even in the cases of diatomic molecules. Several diatomic molecules have been examined[9] such as S_2, F_2, Cl_2,[10] CO, NO, SO, and so on. Two sets of pairs (Ar vs N_2 and Xe vs O_2) have been compared and discussed well. If the ionization potential alone affects the ionization rate, their ionization yields should be the same. The ionization rates of the former pair (Ar and N_2) closely resemble each other, and the ionization of N_2 is understood to be atomic-like. On the contrary, the latter pair (Xe and O_2) shows different rates; O_2 is very hard to ionize compared with Xe. Wells et al. examined the ionization of several diatomic molecules with 1.3 μm,[9] and they concluded that the suppressed ionization features cannot be classified as having exclusively tunneling or multiphoton ionization effects. The suppression of ionization in the case of diatomic molecules has been discussed in terms of molecular alignment along the laser polarization direction,[11] dissociative recombination mechanism,[12] vibrational motion and field-induced bond length changes,[13] the ionization potential based on the amount of screening provided to the outer electrons by the inner electrons (effective charge),[14] and destructive interference of electron emission from the two atomic centers.[15] Ionization theory based on the single active electron approximation applicable to atoms under a strong laser field, especially to rare gases, has been used to explain the ionization rate and/or probability of molecules. They are PPT (Perelomov−Popov−Terentev) theory,[16] ADK (Ammosov−Delone−Krainov) theory,[17] and SFA (strong field approximation) with the related particular KFR (Keldysh−Faisal−Reiss) theory.[18] Due to its simplicity, an analytical approach such as ADK theory is presently applicable to any material with few parameters although the limitations of this theory have been stated in many studies. Strong laser field ionization theory has made rapid progress, and several approaches have been proposed to explain the ionization rates of simple molecules such as MO-PPT (molecular-PPT),[10] MO-SFA (molecular-SFA),[19] and MO-ADK (molecular-ADK).[20] MO-PPT, MO-ADK, and MO-SFA (especially for length gauge) have agreed well with experimental results. However, a general straightforward expression applicable to all diatomic molecules has not yet been discovered. For example, F_2 is regarded as a special case among the diatomic molecules. The ionization behavior is similar to that of a rare gas although suppression was expected by the theory. This is not surprising because fluorine has been found to deviate in many physical properties, and the electron−electron correlation should be taken into account to elucidate the problem. Another model well describes

* To whom correspondence should be addressed. Phone: +81-6-6605-2554. Fax: +81-6-6605-2522. E-mail: tomo@sci.osaka-cu.ac.jp.

10.1021/jp0619989 CCC: $33.50
Published on Web 06/06/2006

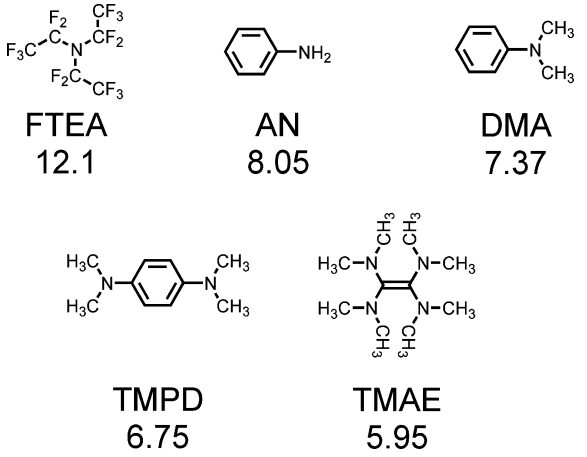

Figure 1. Organic amines ionized by intense femtosecond laser pulses (800 nm, 45 fs): perfluorotriethylamine (FTEA), aniline (AN), *N*,*N*-dimethylaniline (DMA), *N*,*N*,*N*′,*N*′-tetramethyl-1,4-phenylenediamine (TMPD), and tetrakis(dimethylamino)ethylene (TMAE). Abbreviations and vertical ionization potentials are shown below the chemical structures.

the suppressed ionization features for many species by considering their single-photon ionization cross section.[21] The current theoretical development and limitations have been described in ref 22.

Hankin et al. have examined 23 organic molecules with 44 fs pulses at 0.8 μm up to 1×10^{15} W cm^{-2}.[23] They examined molecules with ionization potentials between 8.25 and 11.52 eV. They defined the saturation intensity, I_{sat}, to compare the results of ionization yield between experiments and theory. The ionization rates (yields) of benzene, cyclohexane, and other molecules were generally lower than the values predicted by ADK calculations. We also explored ionization and/or fragmentation of organic molecules[3] under the intensities below 10^{15} W cm^{-2} in addition to the Coulomb explosion of organic molecules below 10^{17} W cm^{-2}.[24] These results were reviewed in refs 25−27. A variety of organic molecules such as aliphatic and aromatic hydrocarbons,[28] halogenated compounds,[3] ketones,[29] and nitro compounds,[30] were examined. To accumulate the knowledge necessary to understand the nature of molecular ionization, it is necessary to examine a variety of molecules with a wide range of ionization potentials.

In this study, we examined several organic amines with very low ionization potentials. They have vertical ionization potential between 5.95 and 12.1 eV. To evaluate the suppressed ionization quantitatively, we measured saturation intensity, I_{sat}, and compared it with that obtained by ADK theory. Deviation from theoretical prediction, i.e., suppression of ionization, was observed in the case of amines; however, the degree of suppression was relatively small compared to that of benzene. The origin of the relatively small suppression ionization is discussed here in terms of the character of the molecular orbital and the screening effect.

Experimental Section

The structure of examined amines are shown in Figure 1. Perfluorotriethylamine (FTEA, PCR, >97%) was dried over calcium hydride followed by distillation. Aniline (AN, Aldrich, >99.5%) and *N*,*N*-dimethylaniline (DMA, Aldrich, >99.5%) were dried over calcium hydride and distilled in vacuum. *N*,*N*,*N*′,*N*′-Tetramethyl-1,4-phenylenediamine (TMPD, Aldrich, 99%) was purified by sublimation. Tetrakis(dimethylamino)-ethylene (TMAE, Tokyo Kasei) was purified as described in the literature[31] and treated under nitrogen atmosphere or in vacuum. The trace amounts of volatile impurities were removed by evaporating them in vacuum before use. Samples were degassed by repeated freeze and thaw cycles before use. Xenon was purchased from Japan Air Gases with the stated purity of 99.99%. The vapor sample was introduced by a leak valve. The sample inlet, except the sample itself, was heated to certain temperature to avoid adsorption to have stable pressure during the experiments. The chamber pressure was monitored 20 cm away from the laser focus point with a cold cathode pressure gauge. The base pressure of the ionization chamber and the time-of-flight chamber was below 5×10^{-7} Pa. The sample pressure in the ionization chamber was kept below 5×10^{-5} Pa during the experiments to avoid the space-charge effect. The pressure of the time-of-flight mass chamber was 10 times below the ionization chamber by differential pumping.

A 0.5 TW all-diode pumped Ti:Sapphire laser (Thales Laser, Alpha 100/XS, < 30 fs, 100 Hz, > 15 mJ, 800 nm, rms stability ~1%) was used in this study. The pulse width was measured by a second-order single-shot autocorrelator (Thales Laser, TAIGA). The laser beam passes through several materials such as a neutral density filter (BK7, 2 mm), a beam splitter (quartz, 1 mm), a focusing lens (quartz, 5 mm), and an ionization chamber window (quartz, 3 mm). The same materials were placed in front of the autocorrelator. Group velocity dispersions introduced by these materials were compensated with the acoustooptic programmable dispersive filters (Fastlite, Dazzler) to have the minimum pulse width. We did not achieve gain-narrowing compensation by Dazzler, and the typical pulse width was 40−45 fs.

A linear mode of reflectron-type time-of-flight mass spectrometer (TOYAMA, KNTOF-1800) was used for ion analysis. The resolution ($m/\Delta m$, fwhm) was 1000 at $m/z = 129$. The output signal from a MCP (Hamamatsu, F4655-11X) was averaged by a digital oscilloscope (LeCroy, Wave Runner 6100, 1 GHz) for 1000 shots or by a multiscaller (Fast Comtec, P7887). A weak signal was amplified by a fast preamplifier (Phillips Scientific 6954, 1.8 GHz, gain 10). The higher sensitivity of MCP for the highly charged ions was corrected. Velocity-dependent[32] correction factors for multiply charged ions were estimated by observing their ion yields at several acceleration voltages. The correction factor was 2 for doubly charged ions. A slit of 500 μm width was located on the extraction plate perpendicular to the laser propagation direction in order to collect the ion that was generated in the most tightly focused point of the laser beam (achieving ion collection from axially symmetric parallel beam geometry).

The direction of laser polarization (800 nm, horizontal, linear polarization) was parallel to the time-of-flight axis. The laser beam was focused into the ionization chamber with a plano-convex quartz lens of 200 mm focusing length. The position of the lens was adjusted to have a maximum signal intensity of the highest charge state of xenon observed (Xe^{4+} or Xe^{5+}). The laser energy was attenuated by the combination of motorized half-wave plate and polarizer before the multipass amplifier. When the laser energy was sufficiently low to avoid induced nonlinear effects such as white light generation and ablation, the laser energy was also attenuated by a reflection-type neutral density filter (Sigma Koki). A part of the laser beam was reflected by a beam splitter at a small incident angle, and the laser pulse energy was measured using an integrating sphere and a calibrated Si pin-photodiode. The actual laser intensity of the linear polarized pulse at the focus was determined by measuring the saturation intensity, I_{sat}, of xenon by the method

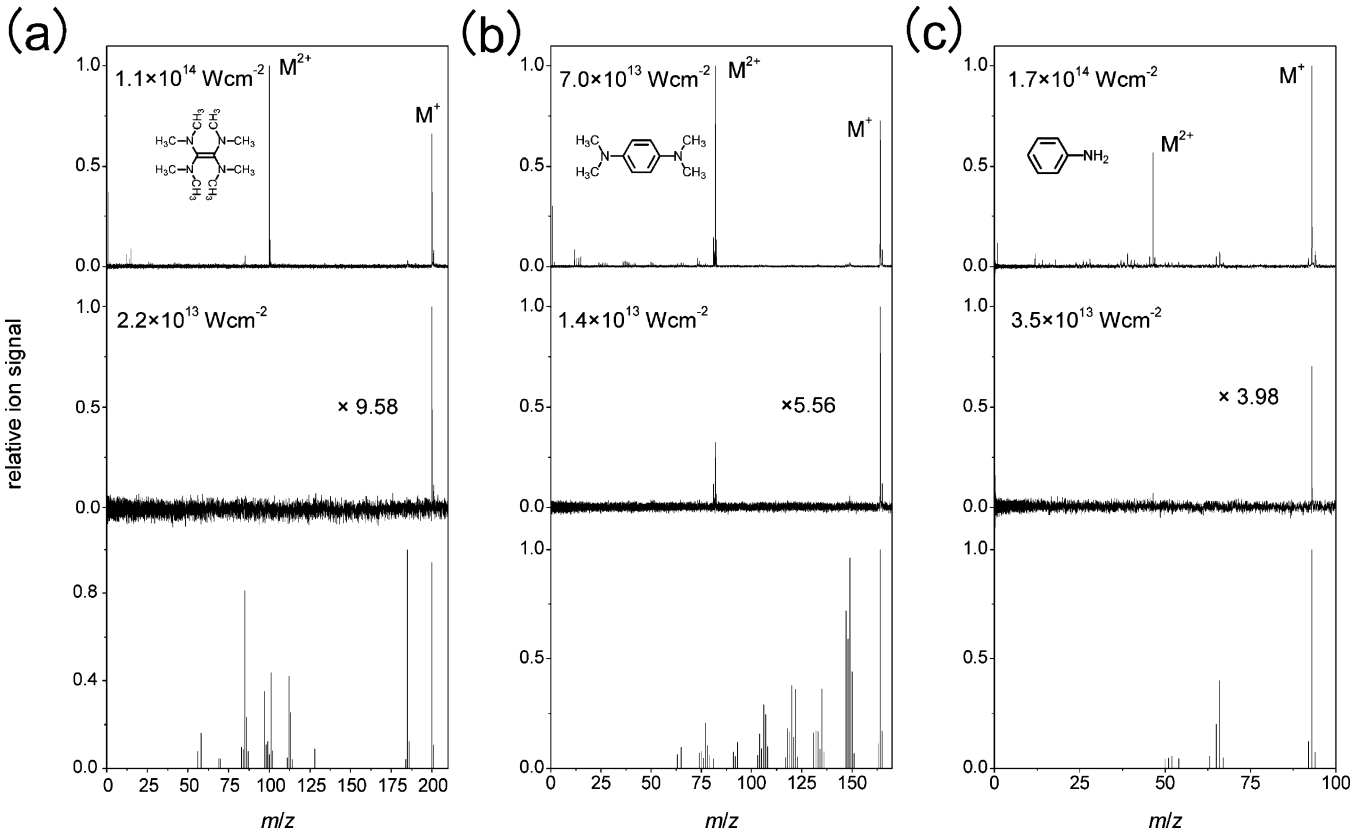

Figure 2. Femtosecond laser ionization mass spectra at two different intensities and electron impact mass spectra (bottom, by GC−MS, Varian SATURN4D, SPB-5, 30 m, 70 eV, 4% cutoff, 50 < *m*/*z*): (a) TMAE, (b) TMPD, and (c) AN. The spectra are taken at around I_{sat} and $5I_{sat}$. The symbol M^{z+} indicates the *z*th charged molecular ion. The original signal intensities are multiplied to provide clearer presentation. The factors are indicated in each column.

of Hankin et al.[23] The saturation intensity of xenon was calculated by ADK theory. In the calculation of saturation intensity, a Gaussian (temporal and spatial) pulse and electron ejection from the p orbital were assumed. We obtained 1.1×10^{14} W cm^{-2} for a 45 fs pulse and used this for intensity calibration. The ions of the amine were measured successively after the measurement of I_{sat} of xenon without, between two runs, changing experimental conditions.

Results and Discussion

Ionization of Amines by Femtosecond Laser Pulses and Their Fragmentation Behavior. Ionization of organic amines was carried out by 45 fs pulses at 0.8 μm. Figure 2 shows the time-of-flight mass spectra of TMAE, TMPD, and AN at different intensities. It is interesting to note that the distribution of fragment ions in the laser ionization mass spectra was different from that in the electron impact mass spectra. The distribution of ions produced by femtosecond laser pulses was much simpler than that produced by electron bombardments.[33] Ions of amines examined in this study were also found in electron impact mass spectra, except for highly charged molecular ions. Significant contribution by highly charged species is a characteristic feature in femtosecond laser ionization mass spectroscopy.[34] For example, ions of m/z = 56, 58, 70, 85, 97, 101, 113, 128, 140, 185, and 200 were found in the electron impact ionization spectrum of TMAE (by GC−MS, Varian SATURN4D, SPB-5, 30 m, 70 eV, 4% cutoff, 50 < *m*/*z*), whereas femtosecond ionization results in ions of m/z = 85, 100, 185, and 200 as shown in Figure 2a. Doubly charged TMAE (m/z = 100) was identified by a noninteger number of isotope peak (m/z = 100.5) and by the peak intensity ratio. Sorgues et al. observed ions of m/z = 73 and 116 for TMAE by a tightly focused femtosecond laser pulse.[35] Contrary to their results, such ions were not observed at any laser intensities in our experiments. We did not use a supersonic beam as they did, but that may not be the reason for the contradiction. TMAE is an exceptionally electron-rich alkene; therefore, it reacts with oxygen very easily. If oxidized products were contaminated, they would appear at a higher laser intensity because they have a higher ionization potential than TMAE. No oxidized products were found by femtosecond laser ionization in our study as shown in Figure 2a. Impurity peaks originating from the oxidation of TMAE such as tetramethylurea (*m*/*z* 116, 72, 44), bis(dimethylamino)methane (*m*/*z* 102, 58), tetramethylhydrazine (*m*/*z* 88, 73, 44, 42), dimethylformamide (*m*/*z* 73, 44), tetramethyloxamide (*m*/*z* 77, cleaved products were observed), and dimethylamine (*m*/*z* 45, 44) were well recognized in the femtosecond laser ionization mass spectrum after the exposure of TMAE to air for a few seconds. Other amines are not very sensitive to oxygen but were treated under a nitrogen atmosphere.

Singly charged molecular ion formation was dominant at the low-laser-intensity regime in all amines examined. As laser intensity increased, both double and dissociative ionization took place. It should first be mentioned that the ionization at 0.8 μm becomes somewhat complicated when we try to compare it with theoretical predictions. Because of heavy fragmentation at the high-intensity regime, the ion yield included a significant amount of fragment ions as well as molecular ions. These fragment ions resulted from thermally dissociative processes, resonant-induced fragmentation,[3] and Coulomb explosion of highly charged ions. Fragmentation of molecular ions induced by the latter two

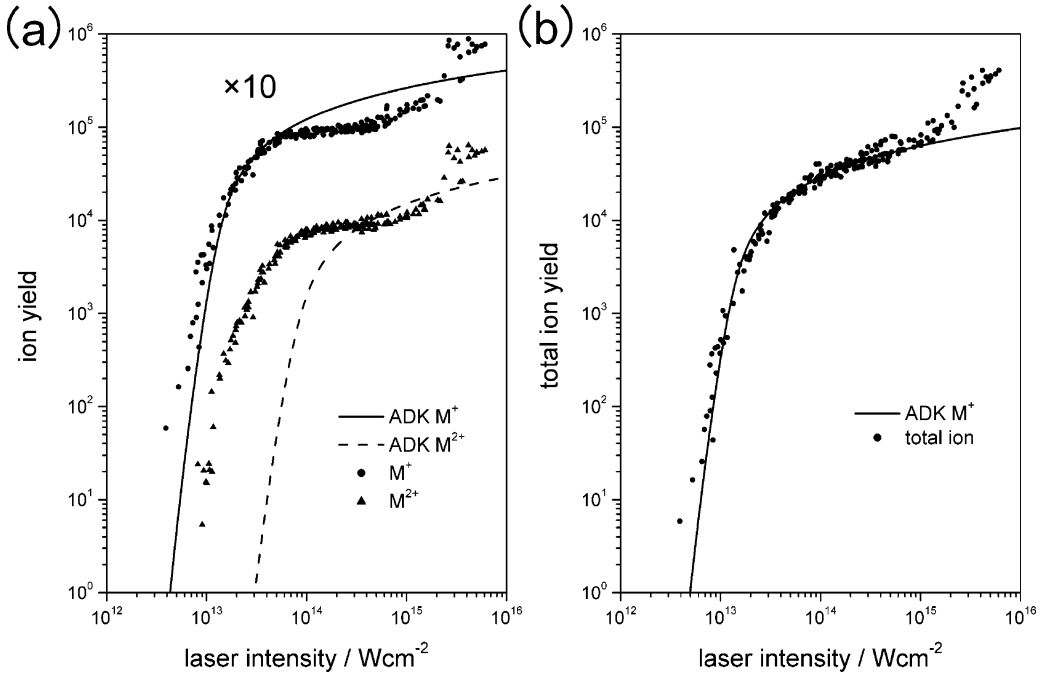

Figure 3. (a) Ion yields of TMPD as a function of laser intensity: singly charged molecular ion (●) and doubly charged molecular ion (▲). The ion yields derived from ADK theory (solid line, singly charged molecular ion; dashed line, doubly charged molecular ion) are also shown. The experimental data and ADK prediction curve of the singly charged molecular ion are multiplied by 10 to provide a clearer presentation. (b) Ion yield of TMPD (total ions) as a function of laser intensity. The solid line is the ADK theory prediction curve for the singly charged molecular ion. The symbol M^{z+} indicates the *z*th charged molecular ion.

processes makes the comparison with theoretical prediction difficult. Neutral amines have no absorption at the laser wavelength, and nonresonant ionization will take place, whereas the resulting radical cation may absorb it. In the case of TMPD, the laser wavelength is not so much overlapped with the cation radical absorption.[36] The TMAE cation is transparent in the visible region.[37] Cation radicals of AN and DMA[38] have absorption at 800 nm; therefore, the resonant-induced fragmentation is expected to occur in those cases. We cannot avoid resonant-induced fragmentation under our experimental conditions. However, the contribution of fragment ions to the total ion yield was relatively smaller than that of molecular ions, even in the cases of AN below the saturation intensity regime. Coulomb explosion is expected to be negligible below the saturation regime. Thus, we count the number of molecular ions (correcting for the higher sensitivity of MCP to doubly charged ions) and fragment ions to obtain a total ion yield. The FTEA molecular ion was not observed at all, as in the electron impact mass spectrum (the ion state may have repulsive potential); therefore, fragment ions were summed to obtain a total ion yield.

Figure 3a shows the ion yields of TMPD as a function of laser intensity. It should be first mentioned that the ionization behavior of TMPD and also that of other amines with low ionization potential was very characteristic. As laser intensity increased, the ion yield increased very steeply until it reached the saturation region ($\sim 3 \times 10^{13}$ W cm^{-2}). After the saturation region, it again increased gently (5×10^{14} W cm^{-2}, approximately). The first slope was 5 and the latter was 1.5 in the case of TMPD. This feature was observed for both singly and doubly charged molecular ions. A similar feature was found in the case of other amines and also in anthracene ($I_P = 7.4$ eV). All ions showed similar features, indicating that this steplike behavior could not be attributed to physical reasons but to experimental issues. A similar step feature could also be found in the earlier experiments without collecting volume restrictions.[39] In such full-volume experiments, in which the whole focal region along the beam propagation axis was exposed to the detector, the ionization yield above saturation intensity (ionization probability is unity) was expected to increase as the Gaussian focal volume grew with the $I^{3/2}$ rate (I represents the laser intensity). An attempt to minimize this volume effect by extracting the ions through a slit smaller than the confocal length was performed in this study. The slope of the saturation region was less than 1.5, indicating that volume restriction was achieved. Figure 4a shows the shape of the molecular ion peak of TMPD at different intensities. The full width at half-maximum of the molecular ion peak as a function of laser intensity is shown in Figure 4b. The width of the molecular ion peak was the same below the saturation region (10 ns corresponds to a mass resolution of 1100). The peak became broader in the saturation region, and a double structure appeared at intensities higher than the saturation region. The double peaks should originate from the spatial distribution of singly charged molecular ions. As the laser intensity increases, a higher charge state is formed at the most intense central part of the laser beam, whereas singly charged ions are produced at the wing of the laser beam. The double peak was also observed in the *Z*-scan experiment along the laser propagation direction.[40] Volume restriction along the laser beam propagation (perpendicular to the ion extraction direction) was successful; however, restriction of the volume along the ion extraction direction could not be achieved by placement of a slit. Simple calculation showed that the 20 ns separation of two peaks at 5.1×10^{15} W cm^{-2} corresponded to 88 μm in space along the ion extraction direction under our spectrometer setting. Confinement of an exact ionization volume and determination of absolute ion yield[41] is difficult under our experimental condition. However, we did not observe this feature in the case of xenon ($I_P = 12.13$ eV) up to 5×10^{15} W cm^{-2}, indicating that the volume restriction by slit failed for certain molecules at certain intensities; thus, we observed an ion yield well below the second increase and used them for further analysis.

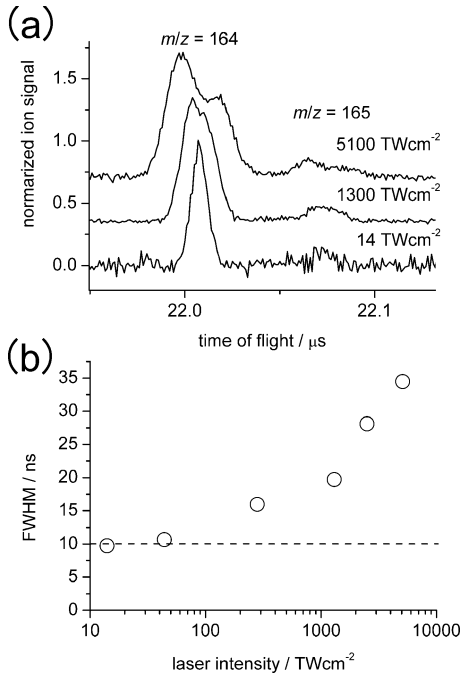

Figure 4. (a) Mass peak of the TMPD singly charged molecular ion at different laser intensities. Spectra are shifted vertically to provide a clearer presentation. (b) Full width at half-maximum (fwhm) of the TMPD singly charged molecular ion peak as a function of laser intensity. The dashed line indicates the spectrometer resolution of 1100.

As clearly seen in Figure 3a, the formation of doubly charged molecular ions was very significant in the case of TMPD. The ratios between doubly charged molecular ions to singly charged ones at the saturation intensity region (TMPD, 2×10^{14} W cm^{-2}) are shown in Table 1. The ratio was exceptionally high in the case of TMPD (0.9). Other amines showed relatively inefficient formation of doubly charged molecular ions. The onset of fragment ion formation and doubly charged ion formation are complementary to each other. The small yield of doubly charged molecular ions may be attributed to inefficient formation, their unstable nature, and resonance-induced fragmentation.

Comparison of Experiment with ADK Calculations. Theoretical approaches to investigating the mechanism of ionization under a strong laser light field are now rapidly developing; however, exact theoretical calculations are presently not applicable to large molecules because the degree of freedom increases rapidly as molecular size increases. The reasons for the difficulty are both structural and dynamical. The multinuclei and multielectron nature of large molecules breaks the spherical symmetry of the electronic wave functions, leading to an increase in complexity. Molecular versions of ionization theories under strong laser fields for several diatomic molecules have been successful by considering the molecular orbitals. However, amines have more complex coordinates, and electron emission was expected from molecular orbitals including nonbonding orbitals; therefore, the extension to this kind of molecule has not presently been in the scope of theoretical consideration. As quantitative theoretical models for large molecules are presently not available, the simple analytical approach of ADK formalism for tunnel ionization was applied in this study, although the limitation of ADK theory has been discussed extensively. ADK theory simply requires the ionization potential and quantum number of electrons for calculation. In the case of atoms and many diatomic molecules, the vertical and adiabatic ionization potential is the same (or similar). However, large molecules have different values due to structural changes (Table 1). Femtosecond laser ionization was considered to be an instantaneous event; therefore, the ionization occurs vertically and we used vertical ionization potential for the calculation. The ionization potential of neutral to doubly charged amines has not been reported previously. We therefore estimated the ionization potential of doubly charged amines as follows. The average energy to form a doubly charged state is 2.65 ± 0.06 times[42] larger than that to form a singly charged state in the cases of aromatic molecules. Thus, we assumed that this value could also be applied to the case of amines. For example, the energy required to ionize singly charged TMPD to a doubly charged state was assumed to be 11.1 eV, and this value was used for the ADK calculation (assuming a sequential ionization process). The ion yield of the experiments and those derived from ADK theory are compared in Figure 3a. Although ADK prediction agreed well with the singly charged ion yield of TMPD, it completely failed to explain (underestimated) the formation of doubly charged molecular ions. It was interesting to note that the same assumption of ionization potential overestimated the doubly charged species in the case of naphthalene ($I_P = 8.15$ eV).[43] Most likely, it was the assumption of ionization energy that failed. Supposing doubly charged molecular ions and fragment ions are formed from singly charged molecular ions, we can compare the total ion in experiments with singly charged ion in the ADK calculation. Figure 3b shows a comparison of the total ion yield, the sum of all ions, of experimental yields, and singly charged molecular ion yield derived from ADK theory. They agreed well with each other except for in the high-intensity region, due to the volume effect discussed earlier.

The ionization took place nonresonantly, and our experimental ion yield was in good agreement with the theoretical value assuming tunnel ionization in the case of TMPD; however, the ionization mechanism was still difficult to identify. Talebpour et al. have studied the ionization of benzene and pyridine using a 200 fs pulse at 800 nm and an intensity range of 4×10^{12} to 2×10^{14} W cm^{-2}.[44] Their results indicated that a multiphoton ionization model can account for the intensity dependence of the ion yields. Due to their low ionization potential, absorption of a few photons can reach the ionization threshold in the case of some amines. They require four photons (TMAE) and five photons (DMA, TMPD), respectively. AN and FTEA have relatively high ionization potentials and need six and eight photons, respectively. The slope at the steep region below saturation was 5 in the case of TMPD, indicating that a multiphoton mechanism could also applicable. Photoelectron spectroscopy would elucidate the problem.

Relatively Small Suppressed Ionization: The Effect of Molecular Structure and Emission of the Electron Belonging to the Lone Pair of Nitrogen. We used the saturation intensity (I_{sat}) proposed by Hankin et al., to evaluate the degree of suppressed ionization quantitatively. I_{sat} corresponds to the intensity at a certain ionization probability, which in turn depends on the ionization mechanism. A typical example of the determination of I_{sat} for total ions is shown in Figure 5a. I_{sat} is defined as the point at which the ion yield (linear scale), extrapolated from the high-intensity linear portion of the curve, intersects the intensity axis (logarithmic scale).[23] Good linear lines were obtained for AN and xenon, and the intersect gave $I_{sat\ exp}$. Figure 5b shows the singly charged molecular ion yield and ionization probability of AN derived from ADK theory. The same procedure was used to determine the theoretical value, $I_{sat\ ADK}$. The I_{sat} of xenon was also used to determine the actual

TABLE 1: Ionization Potentials and Saturation Ionization Intensity (I_{sat}) of Amines

	IP/ eV[a]	IP/ eV[b]	ΔIP/ eV[c]	I_{sat}/TW cm^{-2} $I_{sat\ exp}$[d]	I_{sat}/TW cm^{-2} $I_{sat\ ADK}$[d]	$I_{sat\ exp}/I_{sat\ ADK}$	M^{2+}/M^{+} [e]
perfluorotriethylamine (FTEA)	11.7	12.1[f]		118	110	1.1	
aniline (AN)	7.72	8.05	0.33	33	25.1	1.3	0.45
N,*N*-dimethylaniline (DMA)	7.12	7.37	0.25	25	18.4	1.4	0.17
N,*N*,*N*,*N*-tetramethyl-1,4-phenylenediamine (TMPD)	6.20	6.75	0.55	15	13.2	1.1	0.90
tetrakis(dimethylamino)ethylene (TMAE)	5.36	5.95	0.59	16	8.17	2.0	0.44
xenon	12.13	12.13	0	110	110	1.0	

[a] Adiabatic ionization potential, ref 33. [b] Vertical ionization potential, ref 33. [c] The difference of vertical and adiabatic ionization potentials. [d] $I_{sat\ exp}$ was determined for total ions in experiments. $I_{sat\ ADK}$ was determined for singly charged molecular ions in the ADK calculation. [e] Ratio of the ion yield between doubly charged and singly charged molecular ions at the saturation intensity region (averaged). [f] The vertical ionization potential was evaluated from the adiabatic ionization potential by the relation I_P (vertical) = 0.55 + 0.99I_P (adiabatic). The correlation was deduced from the data of ethylamine, triethylamine, 1-phenylpyrrolidine, 1,4-phenylenediamine, and other amines listed above ($n = 8$, $r^2 = 0.99$).

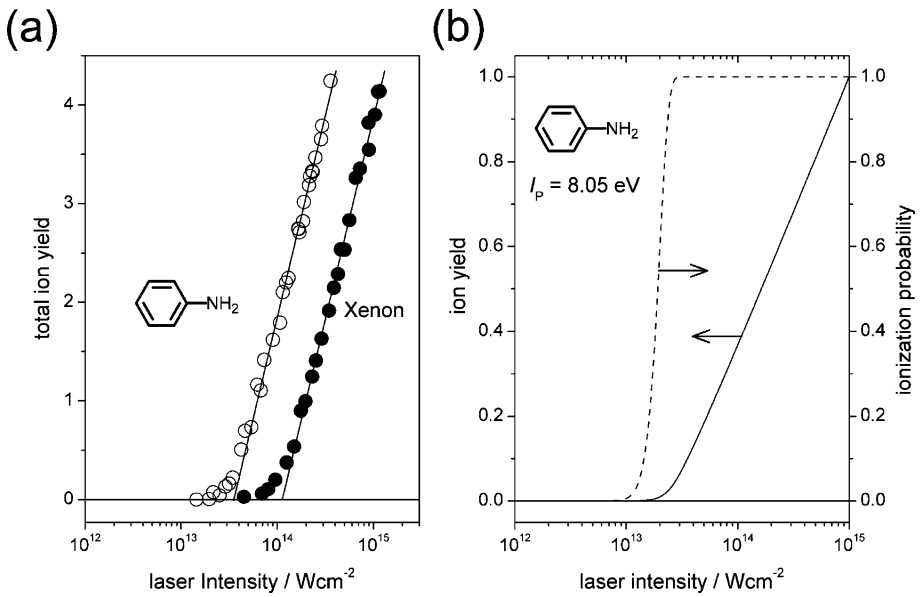

Figure 5. (a) Correlation between the total ion yield (○, AN; ●, Xe) and the logarithm of the laser intensity. The solid linear lines are the extrapolation from the high-intensity linear portion of the plots. The intersection with the intensity axis gives $I_{sat\ exp}$. (b) Ion yield and ionization probability of AN derived from ADK theory as a function of the logarithm of the laser intensity.

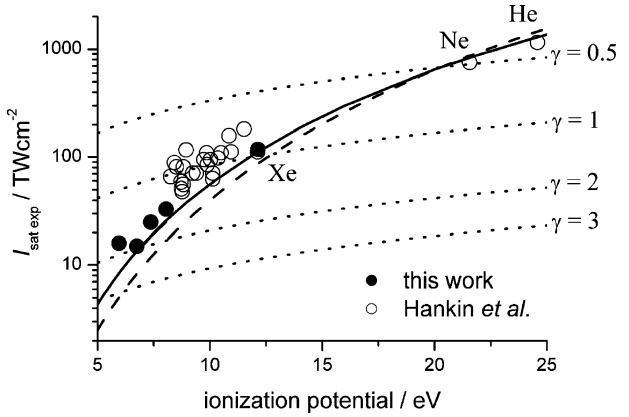

Figure 6. $I_{sat\ exp}$ as a function of ionization potential: amines (●, this study, 0.8 μm, 45 fs) and organic molecules and rare gases (○, ref 23, 0.8 μm, 44 fs). The solid line is the ADK prediction curve, $I_{sat\ ADK}$. The dashed line is the barrier suppression ionization intensity (not I_{sat} value) for comparison. The dotted lines are the curves of the Keldysh parameter γ of certain values indicated.

intensity at the focus (linear polarized pulse). We obtained the actual intensity by fixing the measured $I_{sat\ exp}$ of Xe (the sum of all charge states after the MCP sensitivity correction) to its ADK value, $I_{sat\ ADK}$.

Figure 6 shows the correlation between $I_{sat\ exp}$ and the ionization potential. $I_{sat\ ADK}$, BSI (barrier suppression ionization) intensity,[45] and the Keldysh parameter γ at certain values are also shown (45 fs, 800 nm) in Figure 6. The plots contain the data of 23 organic molecules from ref 23 (44 fs, 800 nm). The I_{sat} values of organic molecules were found between 15 and 180 TW cm^{-2}. These intensities correspond to the γ value between 0.7 and 2. The validity region of tunneling ionization theory in atoms could be deduced by an adiabaticity parameter known as the Keldysh parameter γ.[18] The tunneling ionization theory was valid where γ was smaller than 1. ADK theory was understood to overestimate the ionization rate when γ was larger than 1, because the tunneling time for the electron became much longer than the optical period and the quasistatic approximation failed although the Coulomb barrier was greatly suppressed. On the other hand, the conventional Keldysh parameter based on the Coulomb model and the zero-range potential model was concluded to underestimate the border between the multiphoton ionization and tunneling ionization regimes in the case of large molecules. Even at high γ values, tunneling ionization dominated in aromatic molecules.[46] The adiabaticity parameter based on the molecular electrostatic potential was suggested as a molecular Keldysh parameter.[47] The validity of the original γ value was strongly dependent on the molecular properties. If we intend to compare the ionization rates of molecules with those of rare gases with the same ionization potential, we could use ADK formalism, which well describes the ionization behavior of rare gases. To examine the region where γ is larger

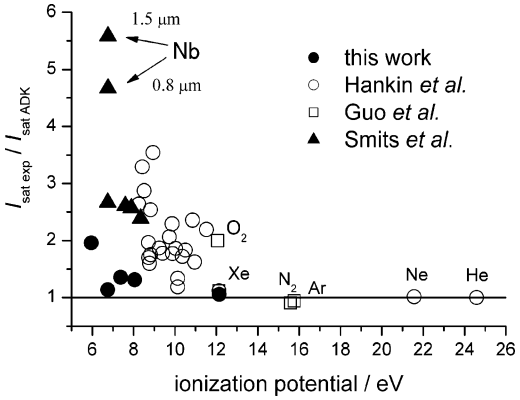

Figure 7. Ratio of the experimental saturation intensity $I_{sat\ exp}$ to the calculated saturation intensity $I_{sat\ ADK}$ as a function of ionization potential: amines (●, this study, 800 nm, 45 fs), organic molecules and rare gases (○, ref 23, 800 nm, 44 fs), singly charged transition metal ions (▲, refs 49 and 50, 1500 nm, 90 fs), diatomic molecules (□, O_2 (O_2^+), N_2 (N_2^+), and Ar (Ar^+), Figures 1 and 2 of ref 14, 800 nm, 30 fs).

than 1, the PPT model was better than the ADK model even in the cases of rare gases.[48] In the case of diatomic molecules, the MO-PPT model successfully described the ionization rate of Cl_2 at $\gamma = 3.5$.[10] We used the ADK theory because deviation in the low-intensity region will not affect the determination of I_{sat}. Apparently, both ADK theory and the BSI model underestimate the $I_{sat\ exp}$; in other words, all molecules showed suppressed ionization nature in comparison with rare gases with the same ionization potential.

Figure 7 shows the ratio between I_{sat} values of experiments ($I_{sat\ exp}$) and of ADK prediction ($I_{sat\ ADK}$) to visualize the suppressed ionization quantitatively. These plots include the data obtained under different experimental conditions: amines (this study, 800 nm, 45 fs), organic molecules (Hankin et al., 800 nm, 44 fs),[23] transition metals (Smits et al., 1500 nm, 90 fs),[49,50] and diatomic molecules (Guo et al., 800 nm, 30 fs).[51] It should first be mentioned that a fair comparison was difficult for the following reasons: (1) I_{sat} depends on what ions are collected (total ion or specific ion species). (2) The absolute laser intensity determination differs (by the I_{sat} of rare gases, focal properties, etc.). Hankin reported the I_{sat} of xenon as 1.12×10^{14} W cm^{-2} (44 fs; the experimental value was determined by the focal parameters) and 1.0×10^{14} W cm^{-2} (ADK calculation). Smits reported the I_{sat} of xenon as 9.5×10^{13} W cm^{-2} (90 fs; the ADK-predicted value was used as the absolute laser intensity). In our case, the I_{sat} of singly charged xenon was derived from the ADK calculation (1.10×10^{14} W cm^{-2}) and used for intensity calibration. (3) Correction of MCP sensitivity for highly charged species will change the results. (4) A wavelength-dependent I_{sat} was reported for all *trans*-decatetraene.[52,53] The I_{sat} of Nb was also wavelength-dependent as shown in Figure 7.[54] Despite the difficulties in comparing absolute values in the experiments, the relative value against the ADK prediction could be used to discern trends.

As clearly seen in the Figures 6 and 7, the ADK predictions for rare gases such as Xe, Ar, Ne, and He were successful at reproducing the experimental results. However, it should be mentioned that only the ionization yield of rare gases was reproduced by the conventional theory. Smits et al. examined the ionization of transition metals of Ni, V, Nb, Ta, and Pd and observed the suppression of ionization (at 1.5 μm, 90 fs)[49,50] relative to the single active electron approximation expectations. The ADK prediction overestimated the experimentally obtained ionization rate, while the zero-range potential model underestimated them. Among transition metals, the data that deviated furthest from the ADK prediction was found in niobium (the ratio was 5.58 by 1.5 μm and 4.67 by 0.8 μm ionization).

Data of frequently compared diatomic molecular pairs (nitrogen and oxygen, Guo et al. 0.8 μm, 30 fs) are also shown in Figure 7. Nitrogen showed good agreement with ADK prediction, whereas oxygen deviated from the ADK prediction. The experimental I_{sat} of oxygen was twice as large as the ADK-predicted value, indicating that the quantitative evaluation of suppressed ionization by the I_{sat} value was not so much sensitive than the direct comparison of raw ionization rate or yield. However, the comparison of raw ionization yields gave us qualitative information about suppressed ionization. The I_{sat} index was useful to see the tendency of ionization behavior for a variety of species quantitatively. The degree of suppressed ionization of many organic molecules examined by Hankin, evaluated by the I_{sat} value, was equivalent to oxygen (ratio = 2.0). Hankin showed that some of the molecules showed large deviations.[23] The five most suppressed molecules (ratio > 2.5) were cyclohexene (3.54), 1,3,5-hexatriene (3.29),[55] 1,3-hexadiene (2.87),[55] 1,3-cyclohexadiene (2.64), and 1,4-cyclohexadiene (2.54),[55] respectively.

The data that deviated furthest from the ADK prediction found in this study was that for TMAE. The I_{sat} value was 2 times higher than the predicted values based on ADK theory. TMPD, which has the second lowest ionization potential (6.75 eV) examined in this study, did not show significant suppressed ionization (ratio = 1.1). Other amines also did not show significant suppressed ionization behavior (ratio < 1.5). It was surprising that the ionization of molecules with very low ionization potential could be described by ADK theory based on a single active electron approximation. It was very important that the degree of suppression was smaller than that of benzene (ratio = 1.9)[23] although all the examined amines except for TMAE and FTEA have a benzene ring. Special attention should be paid to the case of TMAE. The population of intermediate states via multiphoton absorption could be included. TMAE has a weak absorption at 400 nm. Only two photons are necessary to access the diffuse Rydberg state (3s ← N),[56] and an additional two photons are required to reach the ionization continuum with 800 nm pulses (2 + 2 ionization process). If the real excited state was populated, competition between further ionization and ultrafast relaxation of the Rydberg state could have reduced the ionization rate and, as a result, increased I_{sat}.

Recently, electron screening effects have been recognized as an important factor affecting the ionization rate of multielectron systems, such that electron correlation should be taken into account.[57] Supposing that not only outer electrons but also inner electrons were shaken by the external electric field simultaneously, the collective movement of electrons toward one side of the potential well resulted in the repulsion of electrons and increased the potential barrier. As a result, the tunneling of the outer electron was suppressed. The screening effect due to electron correlation would be substantial as the system size becomes larger due to the long-range delocalization of π electrons as observed in decatetraene, etc.,[57] and several dienes which gave large suppression.[23] The origin of suppressed ionization in transition metals was also explained by a screening effect, and it was concluded that a large screening effect results in significant deviation of Nb, which has extremely large polarizabilities. As for the suppression of multiple ionization in the silver dimer, the screening effect due to the cancellation of polarization of the outer s electron (distributed widely and shaken effectively in the direction of the laser polarization) by

the movement of inner d electrons (localized around each silver nucleus) to the opposite direction against the valence s electron was found by TD-DFT calculation.[58] The TD-DFT calculation was applied for model molecules,[59] diatomic molecules,[60] and medium-size molecules such as ethylene and benzene[61] to evaluate the screening effect quantitatively. The growth of the potential barrier caused by the screening effect at 4×10^{13} W cm^{-2} was calculated to be 0.5 eV for ethylene and 2 eV for benzene, respectively. In addition, electron emission from other orbitals besides the highest occupied molecular orbital (HOMO) was recently recognized as an important factor of suppressed ionization in large molecules.[61]

It is possible to state the reason for the rather small (or comparable) suppressed ionization behavior of amines compared to that of benzene. In the case of simple diatomic molecules, the suppression was explained by the orbital symmetry of the HOMO; however, such logic does not apply to large molecules with low symmetry. From the viewpoint of the screening effect, the character of electrons belonging to the highest molecular orbital should be important. The first electron emission of DMA[62] and TMAE[63] is from the π orbital; however, nonbonding orbitals of the nitrogen atom contribute substantially. In the case of TMAE, the HOMO is antibonding between four nitrogens. Suppose electrons are particularly localized on the nitrogen atom(s) and apart from the other π electrons in benzene (or ethylene) moiety; the dynamics of π electrons in the benzene ring (or ethylene) could not affect the ionization of the nonbonding electrons. As a result, the screening effect becomes smaller than (or comparable to) that of benzene. If the electron emission was solely from nonbonding orbitals, the screening effect would be relatively small. The suppression was not significant in the case of FTEA. In addition, we have found that the ionization yield of simple multiatomic molecules such as halogenated methanes can be described by ADK theory within the factor of 1.1 in the I_{sat} scale.[64] In these cases, an electron emission would be expected from a spherical wave function tightly located on a halogen atom. The ionization from a lone pair orbital is presently not in the scope of ionization theory. We hope that these results will stimulate further theoretical consideration of ionization phenomena of large molecules under a strong laser field.

Acknowledgment. The present research was financially supported by a Grant-in-Aid (No. 14077214) from the Ministry of Education, Culture, Sports, Science and Technology, Japan to N.N. We thank Mr. Hervé Jousselin of Thales Laser Co. for his kind contribution to our laser system.

References and Notes

(1) *Molecules and Clusters in Intense Laser Fields*; Posthumus, J., Ed.; Cambridge University Press: Cambridge, 2001.

(2) Harumiya, K.; Kawata, I.; Kono, H.; Fujimura, Y. *J. Chem. Phys*. **2000**, *113*, 8953.

(3) (a) Harada, H.; Shimizu, S.; Yatsuhashi, T.; Sakabe, S.; Izawa, Y.; Nakashima, N. *Chem. Phys. Lett.* **2001**, *342*, 563. (b) Harada, H.; Tanaka, M.; Murakami, M.; Shimizu, S.; Yatsuhashi, T.; Nakashima, N.; Sakabe, S.; Izawa, Y.; Tojo, S.; Majima, T. *J. Phys. Chem. A* **2003**, *107*, 6580.

(4) Markevitch, A. N.; Romanov, D. A.; Smith, S. M.; Schlegel, H. B.; Ivanov, M. Yu.; Levis, R. *J. Phys. Rev. A* **2004**, *69*, 013401.

(5) Robson, L.; Ledingham, K. W. D.; Tasker, A. D.; McKenna, P.; McCanny, T.; Kosmidis, C.; Jaroszynski, D. A.; Jones, D. R.; Lssac, R. C.; Jamieson, S. *Chem. Phys. Lett*. **2002**, *360*, 382.

(6) Campbell, E. E. B.; Hansen, K.; Hoffmann, K.; Korn, G.; Tchaplyguine, M.; Wittmann, M.; Hertel, I. V. *Phys. Rev. Lett.* **2000**, *84*, 2128.

(7) Murakami, M.; Mizoguchi, R.; Shimada, Y.; Yatsuhashi, T.; Nakashima, N. *Chem. Phys. Lett*. **2005**, *403*, 238.

(8) Trushin, S. A.; Fuss, W.; Schmid, W. E. *J. Phys. B* **2004**, *37*, 3987.

(9) (a) Wells, E.; DeWitt, M. J.; Jones, R. R. *Phys. Rev. A* **2002**, *66*, 013409. (b) DeWitt, M. J.; Wells, E.; Jones, R. R. *Phys. Rev. Lett*. **2001**, *87*, 153001.

(10) Benis, E. P.; Xia, J. F.; Tong, X. M.; Faheem, M.; Zamkov, M.; Shan, B.; Richard, P.; Chang, Z. *Phys. Rev.* A **2004**, *70*, 025401.

(11) Talebpour, A.; Larochelle, S.; Chin, S. L. *J. Phys. B* **1998**, *31*, L49.

(12) Talebpour, A.; Chien, C.-Y.; Chin, S. L. *J. Phys. B* **1996**, *29*, L677.

(13) Saenz, A. *J. Phys. B* **2000**, *33*, 4365.

(14) Guo, C. *Phys. Rev. Lett*. **2000**, *85*, 2276.

(15) Muth-Böhm, J.; Becker, A.; Faisal, F. H. M. *Phys. Rev. Lett*. **2000**, *85*, 2280.

(16) Perlomov, A. M.; Popov, V. S.; Terentev, M. V. *Sov. Phys. JETP* **1966**, *23*, 924.

(17) Ammosov, M. V.; Delone, N. B.; Krainov, V. P. *Sov. Phys. JETP* **1986**, *641*, 1191.

(18) (a) Keldysh, L. V. *Sov. Phys. JETP* **1965**, *20*, 1307. (b) Faisal, F. H. M. *J. Phys. B* **1973**, *6*, L89. (c) Reiss, H. R. *Phys. Rev. A* **1980**, *22*, 1786.

(19) (a) Muth-Böhm, J.; Becker, A.; Chin, S. L.; Faisal, F. M. H. *Chem. Phys. Lett*. **2001**, *337*, 313. (b) Kjeldsen, T. K.; Bisgaard, C. Z.; Madsen, L. B.; Stapelfeldt, H. *Phys. Rev. A* **2003**, *68*, 063407.

(20) Tong, X. M.; Zhao, Z. X.; Lin, C. D. *Phys. Rev. A* **2002**, *66*, 033402.

(21) Uiterwaal, C. J. G. J.; Gebhardt, C. R.; Schröder, H.; Kompa, K.-L. *Eur. Phys. J. D* **2004**, *30*, 379.

(22) Usachenko, V. I.; Chu, S.-I. *Phys. Rev. A* **2005**, *71*, 063410.

(23) (a) Hankin, S. M.; Villeneuve, D. M.; Corkum, P. B.; Rayner, D. M. *Phys. Rev. Lett*. **2000**, *84*, 5082. (b) Hankin, S. M.; Villeneuve, D. M.; Corkum, P. B.; Rayner, D. M. *Phys. Rev. A* **2001**, *64*, 013405.

(24) (a) Kou, J.; Nakashima, N.; Sakabe, S.; Kawato, S.; Ueyama, H.; Urano, T.; Kuge, T.; Izawa, Y.; Kato, Y. *Chem. Phys. Lett.* **1998**, *289*, 334. (b) Kou, J.; Zhakhovskii, V.; Sakabe, S.; Nishihara, K.; Shimizu, S.; Kawato, S.; Hashida, M.; Shimuzu, K.; Bulanov, S.; Izawa, Y.; Kato, Y.; Nakashima, N. *J. Chem. Phys.* **2000**, *112*, 5012. (c) Shimizu, S.; Kou, J.; Kawato, S.; Shimizu, K.; Sakabe, S.; Nakashima, N. *Chem. Phys. Lett.* **2000**, *317*, 609. (d) Sakabe, S.; Nishihara, K.; Nakashima, N.; Kou, J.; Shimizu, S.; Zhakhovskii, V.; Amitani, H.; Sato, F. *Phys. Plasmas* **2001**, *8*, 2517. (e) Shimizu, S.; Zhakhovskii, V.; Sato, F.; Okihara, S.; Sakabe, S.; Nishihara, K.; Izawa, Y.; Yatsuhashi, T.; Nakashima, N. *J. Chem. Phys*. **2002**, *117*, 3180. (f) Shimizu, S.; Zhakhovskii, V.; Murakami, M.; Tanaka, M.; Yatsuhashi, T.; Okihara, S.; Nishihara, K.; Sakabe, S.; Izawa, Y.; Nakashima, N. *Chem. Phys. Lett*. **2005**, *404*, 379.

(25) Nakashima, N.; Shimizu, S.; Yatsuhashi, T.; Sakabe, S.; Izawa, Y. *J. Photochem. Photobiol., C* **2000**, *1*, 131.

(26) Nakashima, N.; Yatsuhashi, T.; Murakami, M.; Mizoguchi, R.; Shimada, Y. In *Advances in Multiphoton Processses and Spectroscopy*; Lin, S. H., Villaeys, A. A., Fujimura, Y., Eds.; World Scientific Pub. Co. Inc.: Singapore, 2006; Vol. 17.

(27) Nakashima, N.; Yatsuhashi, T. In *Progress in Ultrafast Intense Laser Science II*; Yamanouchi, K., Chin, S. L., Agostini, P., Ferrante, G., Eds.; Springer, in press.

(28) (a) DeWitt, M. J.; Levis, R. J. *J. Chem. Phys*. **1998**, *108*, 0745. (b) DeWitt, M. J.; Levis, R. J. *J. Chem. Phys*. **1995**, *102*, 8670.

(29) Kosmidis, C.; Tzallas, P.; Ledingham, K. W. D.; McCanny, T.; Singhal, R. P.; Taday, P. F.; Langley, A. J. *J. Phys. Chem. A* **1999**, *103*, 6950.

(30) Tasker, A. D.; Robson, L.; Ledingham, K. W. D.; McCanny, T.; McKenna, P.; Kosmidis, C.; Jaroszynski, D. A. J. *Int. J. Mass Spectrom*. **2003**, *225*, 53.

(31) Holroyd, R. A.; Ehrenson, S.; Preses, J. M. *J. Phys. Chem.* **1985**, *89*, 4244.

(32) (a) Santos, A. C. F.; Melo, W. S.; Sant'Anna, M. M.; Sigaud, G. M.; Montenegro, E. C. *Rev. Sci. Instrum*. **2002**, *73*, 2369. (b) Schram, B.; Boerboom, A.; Kleine, W.; Kistemaker, J. *Proc. Int. Conf. Phenom. Ioniz. Gases, 7th* **1966**, *1*, 170.

(33) NIST Standard Reference Database No. 69 WebBook. http://webbook.nist.gov/chemistry/ (June 2005 release).

(34) Ledingham, K. W. D.; Singhal, R. P.; Smith, D. J.; McCanny, T.; Graham, P.; Kilic, H. S.; Peng, W. X.; Wang, S. L.; Langley, A. J.; Taday, P. F.; Kosmidis, C. *J. Phys. Chem. A* **1998**, *102*, 3002.

(35) Sorgues, S.; Mestdagh, J.-M.; Gloaguen, E.; Visticot, J.-P.; Heninger, M.; Mestdagh, H.; Soep, B. *J. Phys. Chem. A* **2004**, *108*, 3884.

(36) Hirata, Y.; Mataga, N. *J. Phys. Chem*. **1985**, *89*, 4031.

(37) Kuwata, K.; Geske, D. H. *J. Am. Chem. Soc*. **1964**, *86*, 2101.

(38) Shida, T. *Electronic Absorption Spectra of Radical Ions*; Elsevier: New York, 1988.

(39) Augst, S.; Meyerhofer, D. D.; Strickland, D.; Chin, S. L. *J. Opt. Soc. Am. B* **1991**, *8*, 858.

(40) Robson, L.; Ledingham, K. W. D.; McKenna, P.; McCanny, T.; Shimizu, S.; Yang, J. M. *J. Am. Soc. Mass Spectrom*. **2005**, *16*, 82.

(41) Witzel, B.; Schröder, H.; Kaesdorf, S.; Kompa, K.-L. *Int. J. Mass Spectrom. Ion Processes* **1998**, *172*, 229.

(42) Tobita, S.; Leach, S.; Jochims, H. W.; Rühl, E.; Illenberger, E.; Baumgärtel, H. *Can. J. Phys*. **1994**, *72*, 1060.
(43) Yatsuhashi, T.; Nakashima, N. *J. Phys. Chem. A* **2005**, *109*, 9414.
(44) Talebpour, A.; Larochelle, S.; Chin, S. L. *J. Phys. B* **1998**, *31*, 2769.
(45) Augst, S.; Strickland, D.; Meyerhofer, D. D.; Chin, S. L.; Eberly, J. H. *Phys. Rev. Lett*. **1989**, *63*, 2212.
(46) DeWitt, M. J.; Levis, R. J. *J. Phys. Rev. Lett*. **1998**, *23*, 5101.
(47) DeWitt, M. J.; Levis, R. J. *J. Chem. Phys*. **1998**, *108*, 7739.
(48) Larochelle, S. F. J.; Talebpour, A.; Chin, S. L. *J. Phys. B* **1998**, *31*, 1215.
(49) Smits, M.; de Lange, C. A.; Stolow, A.; Rayner, D. M. *Phys. Rev. Lett*. **2004**, *93*, 213003.
(50) Smits, M.; de Lange, C. A.; Stolow, A.; Rayner, D. M. *Phys. Rev. Lett*. **2004**, *93*, 203402.
(51) Guo, C.; Li, M.; Nibarger, J. P.; Gibson, G. N. *Phys. Rev. A* **1998**, *58*, 4271.
(52) Lezius, M.; Blanchet, V.; Rayner, D. M.; Villeneuve, D. M.; Stolow, A. J.; Ivanov, M. Y. *Phys. Rev. Lett*. **2001**, *86*, 51.
(53) Suzuki, M.; Mukamel, S. *J. Chem. Phys*. **2004**, *120*, 669.
(54) Smits, M. Ph.D. Thesis, Vrije Universiteit, The Netherlands, 2005.
(55) The I_{ADK} values in Table 1 of ref 23 were corrected. We performed the ADK calculation to have the I_{ADK} of Xe be 1.0×10^{14} W cm^{-2}.
(56) Nakato, Y.; Ozaki, M.; Tsubomura, H. *Bull. Chem. Soc. Jpn*. **1972**, *45*, 1299.
(57) Lezius, M.; Blanchet, V.; Ivanov, M. Y.; Stolow, A. *J. Chem. Phys*. **2002**, *117*, 1575.
(58) Shiratori, K.; Nobusada, K.; Yabana, K. *Chem. Phys. Lett*. **2005**, *404*, 365.
(59) Kitzler, M.; Zanghellini, J.; Jungreuthmayer, Ch.; Smits, M.; Scrinzi, A.; Brabec, T. *Phys. Rev. A* **2004**, *70*, 041401.
(60) Otobe, T.; Yabana, K.; Iwata, J.-I. *Phys. Rev. A* **2004**, *69*, 053404.
(61) Otobe, T.; Yabana, K. *Abstracts of Papers*, 14th International Laser Physics Workshops, Kyoto, Japan, July 4−8, 2005; p137.
(62) Rozeboom, M. D.; Houk, K. N.; Searles, S.; Seyedrezai, S. E. *J. Am. Chem. Soc*. **1982**, *104*, 3448.
(63) Cetinkaya, B.; King, G. H.; Krishnamurthy, S. S.; Lappert, M. F.; Pedley, J. B. *Chem. Commun*. **1971**, 1370.
(64) Tanaka, M.; Murakami, M.; Obayashi, T.; Panja, S.; Yatsuhashi, T.; Nakashima, N. *Abstracts of Papers*, 21st IUPAC Symposium on Photochemistry, Kyoto, Japan, April 2−7, 2006, p 269.